

Cation Distribution and Interatomic Interactions in Oxides with Heterovalent Isomorphism: VIII.¹ A High-Temperature Study of the Structure of $\text{Gd}_2\text{SrAl}_2\text{O}_7$

I. A. Zvereva, Yu. E. Smirnov, and J. Choisnet

St. Petersburg State University, St. Petersburg, Russia
University of Caen, Caen, France

Received October 10, 2002

Abstract—The interatomic distances and distribution of gadolinium and strontium cations over two positions in the structure of $\text{Gd}_2\text{SrAl}_2\text{O}_7$ at 1273 K were determined by full-profile X-ray diffraction analysis. A comparative analysis was made of the anisotropy of thermal expansion of the coordination polyhedra in layered perovskite-like structures of the $\text{Sr}_3\text{Ti}_2\text{O}_7$ and K_2NiF_4 types.

Double aluminate $\text{Gd}_2\text{SrAl}_2\text{O}_7$ crystallizing in the $\text{Sr}_3\text{Ti}_2\text{O}_7$ structural type (space group $I4/mmm$) belongs to Ruddlesden–Popper phases [2] which are built up in the block fashion from interpenetrating (2/1 junction type) fragments of perovskite (P) and rock salt (RS) structures with the layer alternation sequence ... (P)(P)(RS)(P)(P)(RS).... In the structure of $\text{Gd}_2\text{SrAl}_2\text{O}_7$, the isomorphous Gd^{3+} and Sr^{2+} cations occupy two positions, 2*b* and 4*e*, which are centers of oxygen polyhedra with the coordination numbers 12 [(Gd,Sr) O_{12} cubooctahedra] and 9 [(Gd,Sr) O_9 monocapped distorted tetragonal antiprisms] (Fig. 1). It is commonly considered that the former positions are located in double perovskite layers (P)(P), and the latter, in rock salt layers.

Data on interatomic distances and distribution of rare-earth cations and strontium over two positions in aluminates $\text{Ln}_2\text{SrAl}_2\text{O}_7$ (Ln = La, Nd, Gd) at room temperature were obtained previously [3]. It was shown that the occupancy of the (Ln,Sr) O_{12} cubooctahedra with the Sr^{2+} cations and that of the (Ln,Sr) O_9 nonahedra with the Ln^{3+} cations grow in the series La, Nd, Gd. The conclusions were based both on direct occupancy calculations and on analysis of variation of the interatomic distances.

In this work, using full-profile X-ray diffraction analysis followed by Rietveld refinement of the structural parameters, we obtained crystal-chemical data for $\text{Gd}_2\text{SrAl}_2\text{O}_7$ at 1273 K. The results of structural

calculations for this temperature and the data obtained previously for room temperature are listed in Tables 1 and 2. It is seen that the parameters and volume of the $\text{Gd}_2\text{SrAl}_2\text{O}_7$ unit cell increase with temperature. The coefficient of thermal expansion (β), calculated assuming linear variation of the parameters in the range 293–1273 K, $\beta = 1/3(2\beta_a + \beta_c) = 9 \times 10^{-6} \text{ K}^{-1}$, is close to those determined for YCaAlO_4 and YCaCrO_4 , 10×10^{-6} and $9 \times 10^{-6} \text{ K}^{-1}$, respectively (here β_a and β_c are the values of β along periods *a* and *c*). The oxides YCaAlO_4 and YCaCrO_4 have the 1/1 type of the layer junction, ... (P)(RS)(P)(RS)...., and crystallize in the K_2NiF_4 structural type [4–7].

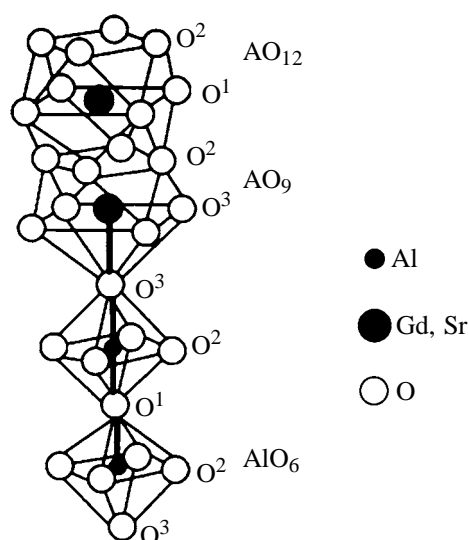


Fig. 1. Coordination polyhedra AlO_6 , $(\text{Gd,Sr})\text{O}_9$, and $(\text{Gd,Sr})\text{O}_{12}$ in the structure of $\text{Gd}_2\text{SrAl}_2\text{O}_7$.

¹ For communication VII, see [1].

Table 1. Unit cell parameters a and c (Å), unit cell volume V (Å³), atomic coordinates (x , y , z),^a thermal parameters B (Å²), and structural (R_B) and profile (R_P) divergence factors (%) for Gd₂SrAl₂O₇ at 293 and 1273 K

Parameter	293 K	1273 K
a	3.7052(2)	3.73149(6)
c	19.781(1)	19.9857(4)
V	271.56	278.28
(Gd,Sr) × 2		
z	0.5	0.5
B	0.37(3)	1.30(8)
(Gd,Sr) × 4		
z	0.3186(2)	0.3188(1)
B	0.37(1)	0.59(4)
Al × 4		
z	0.0942(4)	0.0952(4)
B	0.31(3)	0.37(14)
O ₁ × 4		
z	0	0
B	2.3(1)	2.8(1)
O ₂ × 8		
z	0.1006(5)	0.0992(5)
B	0.65(2)	2.1(1)
O ₃ × 2		
z	0.2035(7)	0.1981(6)
B	0.42(5)	3.4(1)
R_B	3.8	5.0
R_P	5.8	14.7

^a $x = y = 0$ for all the indicated atoms.

Table 2. Occupancies of the oxygen polyhedra in Gd₂SrAl₂O₇

Distribution	(Gd,Sr)O ₁₂ cubo-octahedron		AO ₉ antiprism	
	Gd ²⁺	Sr ²⁺	Gd ³⁺	Sr ²⁺
293 K, experiment	0.28	0.72	0.86	0.14
1273 K, experiment	0.29	0.71	0.855	0.145
Random, calculation	0.67	0.33	0.67	0.33

Table 1 shows that the atomic coordinates, measured in fractions of unit cell period, are similar at both temperatures. The only interesting feature is that at 1273 K the deviation of the Al atom from the $4 \times O^2$ plane becomes less pronounced (the difference between the z coordinates of Al and O² decreases). The out-of-proportion variation of the z coordinate for the “light” and “heavy” atoms indicates that the light atoms show a greater tendency to shift along the

c axis, whereas the positions of the heavy atoms (Gd³⁺, Sr²⁺) are more stable. The parameters of thermal vibrations of atoms (B), as expected, grow with temperature. The highest values of B are observed for the axial oxygen atoms (O¹, O³); the vibrations of the O³ atoms linking the P and RS fragments increase to the greatest extent.

The occupancies of the structural positions with the Gd and Sr atoms (Table 2), calculated for room temperature and 1273 K, virtually coincide. This means that the cation distribution attained in the course of synthesis at 1273 K for 100 h does not noticeably change in the course of recording of the diffraction pattern (10 h). The preferential occupation of the (Gd,Sr)O₉ antiprisms with the gadolinium cations and of the (Gd,Sr)O₁₂ cubo-octahedra with the strontium cations is due to their different ionic radii [8]: Smaller atoms tend to occupy smaller polyhedra. The same trend was observed previously in Ln₂SrAl₂O₇ [3], and also in substitution of calcium for strontium in La₂SrAl₂O₇ [9] and Nd₂SrAl₂O₇ [10]. Namely, as the lanthanide ionic radius decreases in the series La–Nd–Gd, the probability of occupation of the antiprisms with the Ln ions and of the oxygen cubo-octahedra with the Sr ions increases. In La₂SrAl₂O₇, in which the difference between the Ln and Sr ionic radii is the smallest, the distribution of the isomorphous cations is the closest to the random distribution. In Nd₂SrAl₂O₇ and Gd₂SrAl₂O₇, the occupancies of the (Ln,Sr)O₁₂ polyhedra with the lanthanide atoms are smaller than those at random distribution (0.67): 0.54 and 0.28, respectively. In La₂Sr_{1–x}Ca_xAl₂O₇ solid solutions, the calcium ions, being smaller than the lanthanum and strontium ions, occupy the (La,Sr)O₉ polyhedra only. On the contrary, in Nd₂Sr_{1–x}Ca_xAl₂O₇ solid solutions, the ionic radius of Nd is somewhat smaller than that of Ca, and in this case the calcium ions occupy the (Nd,Sr)O₉ polyhedra preferentially but not exclusively.

The temperature changes in the interatomic distances are given in Table 3. It is seen that not all the bond lengths increase with temperature. The greatest difference between the A–O bond lengths, $\Delta(A-O)$, both at room temperature and at 1273 K, is observed in the (Gd,Sr)O₉ antiprism, and the smallest difference, in the (Gd,Sr)O₁₂ cubo-octahedra. In AlO₆ distorted oxygen octahedra forming double layers perpendicular to the c axis, the Al–O interactions are also essentially anisotropic. The aluminum atoms are shifted from the plane of equatorial O² atoms toward the axial O¹ atom (see z coordinates in Table 1).

The length of the equatorial Al–O² bonds regularly increases with temperature, although the mean length

of the Al–O bond in the octahedra remains virtually unchanged. The character of distortion of the octahedra at 293 and 1273 K is different, as indicated by the coefficients of tetragonal distortion α_1 – α_3 ; at 1273 K, the AlO_6 octahedra are the least distorted (Table 3). On heating, the lengths of the axial bonds Al–O^1 and Al–O^3 become closer to each other at the expense of shortening of the latter bond linking the P and RS layers; as a result, the thickness of the double perovskite layer PP ($\text{O}^3\text{–Al–O}^1\text{–Al–O}^3$) decreases also. The bond competition in the $\text{A–O}^3\text{–Al}$ chain linking the P and RS layers leads to considerable lengthening of the A–O^3 bond against the background of shortening of the Al–O^3 bond. As a result, the length of the $\text{A–O}^3\text{–Al}$ chain is not very sensitive to temperature.

The interatomic distances in the AO_{12} cubooctahedra are affected by temperature most weakly; in these fragments, variations of the lengths of all the bonds are the most regular. However, specifically the presence of the AO_{12} cubooctahedra in the layered structure of the $\text{Sr}_3\text{Ti}_2\text{O}_7$ type (2/1 junction) is responsible for the differences between the changes occurring with temperature in the AlO_6 and AO_9 polyhedra, on the one hand, and in K_2NiF_4 -type structures (1/1 junction), on the other hand. A decrease in the distortion of the AO_{12} cubooctahedra results in more significant changes in the axial bond lengths in the octahedra (Table 3), compared to the aluminate of the K_2NiF_4 structure. Table 3 compares data for YCaAlO_4 at room temperature and at 1273 K. In the structure of YCaAlO_4 , the distortion of the AlO_6 and AO_9 polyhedra also decreases with increasing temperature (Fig. 2). All the bonds in the antiprism become longer, and in the octahedron (Fig. 2) the

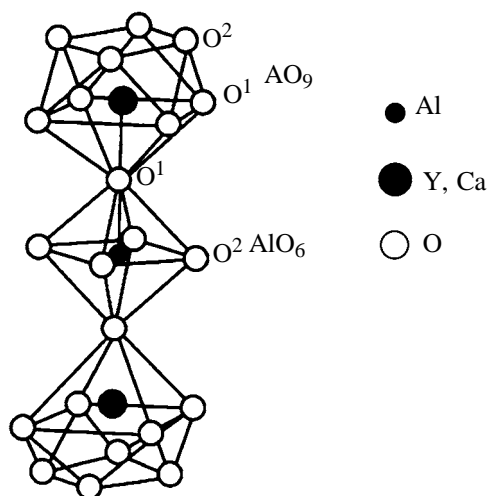


Fig. 2. Coordination polyhedra AlO_6 and $(\text{Y,Ca})\text{O}_9$ in the structure of YCaAlO_4 .

Table 3. Interatomic distances (Å) and parameters Δ and α (for comments, see text) characterizing distortion of the oxygen polyhedra in $\text{Gd}_2\text{SrAl}_2\text{O}_7$ and YCaAlO_4 at 293 and 1273 K ($\text{A} = \text{Gd}, \text{Sr}$ or Y, Ca)

Parameter	$\text{Gd}_2\text{SrAl}_2\text{O}_7$		YCaAlO_4	
	293 K	1273 K	293 K	2273 K
AO_{12} cubooctahedron				
$\text{A–O}^1 \times 4$	2.619(5)	2.639(1)	–	–
$\text{A–O}^2 \times 8$	2.713(6)	2.723(7)	–	–
$\text{A–O}_{\text{av}} \times 12$	2.682	2.695	–	–
$\Delta(\text{A–O})$	0.106	0.084	–	–
AO_9 antiprism				
$\text{A–O}^3 \times 1$	2.292(11)	2.401(13)	2.256(6) ^a	2.301(8) ^a
$\text{A–O}^3 \times 4$	2.653(1)	2.659(2)	2.595(2) ^a	2.613(3) ^a
$\text{A–O}^2 \times 4$	2.451(5)	2.489(7)	2.484(1)	2.515(2)
$\text{A–O}_{\text{av}} \times 9$	2.523	2.555	2.508	2.535
$\Delta(\text{A–O})$	0.361	0.258	0.339	0.312
AlO_6 octahedron				
$\text{Al–O}^3 \times 1$	2.146(12)	2.057(15)	–	–
$\text{Al–O}^1 \times 1$	1.863(6)	1.901(7)	1.993(6)	1.987(9)
$\text{Al–O}^2 \times 4$	1.853(1)	1.868(1)	1.822(1)	1.837(1)
$\text{Al–O}_{\text{av}} \times 6$	1.903	1.905	1.879	1.887
$\Delta(\text{Al–O})$	0.293	0.189	0.171	0.150
$\alpha_1 = \text{Al–O}^3/\text{Al–O}^1$	1.15	1.08	–	–
$\alpha_2 = \text{Al–O}^1/\text{Al–O}^2$	1.01	1.02	1.09	1.08
$\alpha_3 = \text{Al–O}^3/\text{Al–O}^2$	1.16	1.10	–	–
$\text{A–O}^3\text{–Al}$	4.438	4.458	4.249 ^a	4.288 ^a
$\text{Al–O}^1\text{–Al}$	3.726	3.802	–	–
$\text{O}^3\text{–Al–O}^1\text{–Al–O}^3$	8.018	7.916	–	–

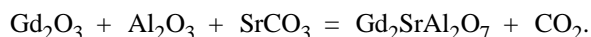
^a The O^3 position in YCaAlO_4 coincides with the O^1 position.

equatorial Al–O^2 bonds become longer, whereas the length of the axial bonds remains virtually unchanged. In the antiprism, the length of the axial A–O^3 bond increases to a considerably greater extent than the lengths of the equatorial A–O^3 bonds. As a result, at high temperature in $\text{Gd}_2\text{SrAl}_2\text{O}_7$ the AO_9 polyhedron becomes less distorted than in YCaAlO_4 , whereas at room temperature the relationship is opposite. This is due to existence of several coordination polyhedra (AO_{12} , AO_9 , AO_6) linked in a common chain along the c -axis (Fig. 1) and to competition of the metal–oxygen bonds, especially in junction of the octahedra and nonahedra. As a result, the bond lengths in different polyhedra vary with temperature differently, and distortion of all the polyhedra noticeably decreases.

In layered oxides of the $\text{Sr}_3\text{Ti}_2\text{O}_7$ and K_2NiF_4 types, the anisotropy of chemical bonds is always due to strains arising when the layers of perovskite and rock salt structures, exhibiting a noticeable geometric mismatch, come in junction [11]. The problems arising at mutual penetration are overcome by distortion of the AlO_6 octahedra and AO_9 polyhedra (due to simultaneous lengthening of Al–O bonds and shortening of axial A–O bonds). Heating partially eliminates these distortions, and in $\text{Sr}_3\text{Ti}_2\text{O}_7$ -type structures bond length leveling is more pronounced than in K_2NiF_4 -type structures.

EXPERIMENTAL

The triple oxide $\text{Gd}_2\text{SrAl}_2\text{O}_7$ was prepared by the ceramic technique from gadolinium oxide, aluminum oxide, and strontium carbonate taken in the proportions corresponding to the reaction equation



The thoroughly mixed charge was pelletized and calcined in corundum crucibles in air for 2 h at 1173 K and then for 100 h at 1723 K.

The X-ray diffraction patterns were taken on a Siemens D-500 diffractometer (CuK_α radiation) equipped with an Antonpar high-temperature attachment, in the 2θ range from 20° to 120° (0.04° step, counting time 12 s) at 1273 K. The unit cell parameters, atomic coordinates, and interatomic distances were determined in the $I4/mmm$ space group from the full profile of the diffraction patterns, with subsequent Rietveld refinement [12, 13].

ACKNOWLEDGMENTS

The study was financially supported by the Russian Foundation for Basic Research (project no. 00-03-

32567) and Competitive Center for Basic Natural Science (project no. E 02-5.0-153).

REFERENCES

1. Smirnov, Yu.E. and Zvereva, I.A., *Zh. Obshch. Khim.*, 2003, vol. 73, no. 2, p. 182.
2. Ruddlesden, S.N. and Popper, P., *Acta Crystallogr.*, 1958, vol. 11, no. 1, p. 54.
3. Zvereva, I.A., Smirnov, Yu.E., Vagapov, D.A., and Choynet, J., *Zh. Obshch. Khim.*, 2000, vol. 70, no. 12, p. 1957.
4. Choynet, J., Archaimbault, F., Crespin, M., Chezhina, N., and Zvereva, I., *Eur. J. Solid State Inorg. Chem.*, 1993, vol. 30, no. 4, p. 619.
5. Zvereva, I., Zueva, L., Archaimbault, F., Crespin, M., Choynet, J., and Lecompt, J., *Mater. Chem. Phys.*, 1997, vol. 48, no. 2, p. 101.
6. Odier, P., Nigara, Y., Coutures, J., and Sayer, M., *J. Solid State Chem.*, 1985, vol. 56, no. 1, p. 32.
7. Berjoan, R., Coutures, J., LeFlem, G., and Saux, M., *J. Solid State Chem.*, 1982, vol. 42, no. 1, p. 75.
8. Shannon, R.D., *Acta Crystallogr., Sect. A*, 1976, vol. 32, no. 5, p. 751.
9. Zvereva, I., Smirnov, Yr., and Choynet, J., *Int. J. Inorg. Mater.*, 2001, vol. 3, no. 1, p. 95.
10. Zvereva, I.A., Seitablaeva, S.R., and Smirnov, Yu.E., *Zh. Obshch. Khim.*, 2003, vol. 73, no. 1, p. 35.
11. Choynet, J., *J. Solid State Chem.*, 1999, vol. 147, no. 2, p. 379.
12. Rietveld, H., *Appl. Crystallogr.*, 1969, vol. 2, no. 1, p. 65.
13. Rodriguez-Carvajal, J.L., *Physica B*, 1992, vol. 192, no. 1, p. 55.